A Case Study of a Small Ovarian Teratoma: Histological and Molecular Characteristics

Shinichi Teshima (steshima@shonankamakura.or.jp)
Shonan Kamakura General Hospital
Urara Sakurai
Musashino Red Cross Hospital
Hirohisa Kishi
Doai Memorial Hospital
Junko Itoh
Shonan Kamakura General Hospital
Hiroyuki Yanai
Okayama University
Ryo Yano
Musashino Red Cross Hospital
Kazuya Onuma
Shonan Kamakura General Hospital
Masayuki Noguchi
Tsukuba University

Case Report

Keywords: Differentiation, Germ layers, Hybridization, In situ, Ovary, RNA, SHH, SOX2, Teratoma

Posted Date: June 23rd, 2022

DOI: https://doi.org/10.21203/rs.3.rs-1437014/v2

Abstract

Background: Ovarian teratomas are ovarian tumors composed of three germ layers. They are rarely detected early, and the early stages have neither been reported often nor well characterized.

Case presentation: We describe a teratoma measuring 2 × 0.8 mm, one of 1254 consecutive ovarian teratomas diagnosed at three institutions. This is the smallest ovarian teratoma reported in the available literature in English. The teratoma bud contained primitive glandular structures, mesoderm-like cells, cord- and sinus-like structures, and surface cells that were flat-to-cuboidal. To characterize this small teratoma, RNA sequencing was performed; 60 RNAs involved in embryonic morphogenesis were detected. The genes *SHH*, *SOX2*, and *SOX9*, which are involved in maturation and differentiation of the early embryo, were expressed in the tumor and evaluated with RNA *in situ* hybridization. We found distinct expression patterns corresponding to the histological components of the teratoma bud that were identified in formalin-fixed paraffin-embedded sections.

Conclusions: The results of the histological and molecular analyses indicated that ovarian teratomas contain rudimentary organ-like features in the early stage of development, and as the tumor grows, these components differentiate into well-developed somatic tissues through the co-expression of RNAs involved in embryonic morphogenesis.

Background

Ovarian teratomas (OTs) are among the most common ovarian neoplasms, accounting for 15% of all ovarian tumors. They are subdivided into mature (95%) and immature teratomas (5%) [1, 2]. OTs are thought to originate from germ cells, arising from abnormal oocytes due to meiotic failure, and grow into pluripotent stem cells that may differentiate into various somatic tissues in three germ layers. However, to date, few reports about stem cells of OT have been published [3].

On average, OTs are 5–10 cm in diameter when detected, and reports of those with diameters of ≤ 5 mm are extremely rare [1, 2, 4]. Due to speculation that small OTs are not easily identifiable because they do not have matured into three germ layers, we have studied OTs with diameters of ≤ 5 mm.

Case Presentation

The patient was a 21-year-old woman who underwent bilateral ovarian cystectomies for bilateral OTs (5 × 5 cm on the left ovary and 6 × 6 cm on the right ovary). The tumors were fixed in 10% formalin, embedded in paraffin, and stained with hematoxylin and eosin. Histologically, the left-sided tumor was diagnosed as an immature teratoma, grade 1, and was composed of three mature germ layers with small foci of neuroepithelial tubules; therefore, left oophorectomy was performed. In the resected left ovary (3 × 2 cm), another 2 × 0.8 mm tumor was detected in the cortex, away from the surgical margin, which appeared to be an OT bud. The right-sided tumor was a mature teratoma, and so the right ovary was preserved. In the > 3 years since, the patient has been disease-free.

The patient provided informed consent for the publication of her case. The study overall conformed the ethical guidelines of the Declaration of Helsinki (revised in 2013). Ethical approval for this case report was obtained from the Institutional Review Board of Musashino Red Cross Hospital, Shonan Kamakura General Hospital and Doai Memorial Hospital.

Histological findings

In the 3 × 2 cm left ovary, an OT bud (width, 2 mm; height, 0.8 mm) was found protruding on the inner surface of the atretic follicle, which was 9 mm in diameter (Figs. 1 and 2). The OT comprised two nodules, 0.6 × 0.8 mm and 1.3 × 0.8 mm in size, which touched each other. No tumor was found in the adjacent 5-μm section.

The OT bud exhibited several rudimentary organ-like features resembling those of an early human embryo (Fig. 2). Two primitive glandular structures were observed inside the tumor; the structure in the upper portion of the tumor had a cystic shape and consisted of dense and overlapping high columnar cells and one layer of flat cells, whereas the structure in the lower portion had an elongated, tubular shape with dense columnar cells, and the center was narrowed and bent. The area around these two structures was composed of small, mesoderm-like, spindle-shaped to cuboidal cells. These cells had densely and sparsely distributed parts. Cord-like arrangements were seen mixed with these mesoderm-like cells. Spindle cells forming sinus-like structures that contained blood cells were also observed. The surface of the two nodules was covered with one layer of cells that were flat-to-cuboidal. These tumor cells showed no evidence of nuclear atypia. Components of the three germ layers of the gonads, neuroepithelial tubules, trophoblast giant cells, and embryonal carcinoma cells were not observed in this OT.

RNA in situ hybridization

RNA *in situ* hybridization (ISH) revealed three representative genes (*SHH*, *SOX2*, and *SOX9*) involved in maturation and differentiation whose levels of expression differed (Figs. 3 and 4). *SHH* was highly expressed in approximately 33% of the upper primitive glandular structure and in 75% of the lower one. Cord-like arrangements also stained strongly in the gene probe. However, *SHH* expression was not confirmed in the mesoderm-like cells or in the flat-to-cuboidal surface cells (Fig. 3a–c). *SOX2* was widely distributed in the two glandular structures with medium to high intensity (Fig. 4a–c). Although both *SHH* and *SOX2* were co-expressed in parts of those structures, the right side of the lower structure, which showed high expression of *SOX2*, did not hybridize with the *SHH* probe (Figs. 3c and 4c). Low signals of *SOX9* were detected on the flat-to-cuboidal surface cells and mesenchymal mesoderm-like cells (Fig. 4d–f). *SOX9* was clearly detected in the sinus-like structures with medium intensity, which also hybridized with the *SHH* probe (Figs. 3b and 4d–f).

Signals of these three RNA probes were completely absent in the normal ovarian tissues around the OT. Immunohistochemistry results for neurofilament protein and glial fibrillary protein were negative (data not shown).

Review of Cases

For this report, we reviewed 1254 consecutive OTs diagnosed at Musashino Red Cross Hospital (Musashino, Japan), Shonan Kamakura General Hospital (Kamakura, Japan), and Doai Memorial Hospital (Tokyo, Japan), and we describe one that manifested as an OT bud, 2 × 0.8 mm in size. To characterize the OT bud, we performed RNA sequencing, and to evaluate the expression of genes involved in embryogenesis, we used RNA ISH.

Specimen Preparation

The 2 × 0.8 mm tumor was embedded in paraffin after formalin fixation and cut serially once into 50 5-μm sections for histological observations, RNA extraction, and RNA ISH. These serial sections were labeled as slides 1–50 and preserved at 4°C until use (Figs. 2–4). The tumor components of three unstained formalin-fixed paraffin-embedded (FFPE) sections (slides 26–28) were scraped with a needle tip, and the RNeasy FFPE kit (QIAGEN, Hilden, Germany) with deparaffinization steps [5] was used to extract the RNA. For the experimental control, RNA was similarly extracted from the normal parts of the same slides where they did not contain oocytes (Fig. 1). The quality of RNA was assessed with Agilent Bioanalyzer High Sensivity RNA Analysis kit (Agilent Technologies, Santa Clara, CA, USA). Since the value of RNA integrity was low, the QIAseq Ultralow Input Library Kit (QIAGEN) was used for sequencing, and 30 million reads of RNA were obtained from both tissues.

To perform RNA sequencing (2 × 36 bases paired-end sequencing), we used NextSeq500 (Illumina, San Diego, CA, USA), which showed that 813 genes were expressed more strongly in the OT sample than in the surrounding ovarian tissue. Sixty genes involved in embryonic morphogenesis were identified by low-expression gene filtering and by Metascape [6, 7]. Three of these genes, *SHH*, *SOX2*, and *SOX9*, were selected for RNA ISH of the tumor. Each of these three genes is well known to be involved in the differentiation and maturation of the early human embryo [8–11]. *SHH* encodes Sonic hedgefog which is a key mediator of anterior–posterior embryonic structures and is expressed in several sites during embryogenesis, where it helps direct the development of neighboring tissues, including the primitive node, notochord, and the floor plate of the neural tube [8, 9, 11]. *SOX2* and *SOX9* encode important transcription factors that regulate the expression of genes that control cellular differentiation during early embryonic stages [9–11].

RNA ISH was performed to localize *SHH*, *SOX9*, and *SOX2* in FFPE tissues of the OT. To obtain specific signals but not background noise from nonspecific hybridization, we used RNAscope™ (Advanced Cell Diagnostics, Newark, CA, USA) as described by Wang et al. [12]. Theoretically, sequential hybridizations with the preamplifier, amplifier, and label probe can enable the visualization of single molecules within each RNA dot plot. The probes used were RNAscope™ Target Probe-Hs-SHH, RNAscope™ Target Probe-Hs-SOX2, and RNAscope™ Target Probe-Hs-SOX9.

Discussion And Conclusions

We have described a very small (2 × 0.8 mm) OT. When detected, OTs usually vary in size from very small (0.5 cm) to large (more than 40 cm); approximately 60% measure between 5 and 10 cm. Histologically,

many of them are mature teratomas composed of three germ layers. Descriptions of the histological features of small OTs (< 1 cm in diameter) have been published [4, 13–15].

The histological features of the small OT in this study greatly differed from those of larger OTs, and it contained structures that resemble those in early embryos (Fig. 2). Therefore, this tumor had to be distinguished from metastasis or residue of the other left-sided OT (5 × 5 cm), which was an immature grade 1 teratoma.

The tumor also differed from various microscopic tumors and tumor-like lesions, such as sex cord tumor with annular tubules (SCTAT), gonadoblastoma, small-sized adenofibroma, SCTAT-like abnormal follicle, multiovular follicle, endometriosis, and germinal inclusion cyst [16], in that it contained rudimentary organ-like features of the early embryo, as shown by histological and molecular pathological studies. The tumor may also resemble the early stage of ovarian (ectopic) pregnancy histologically, except that the latter is surrounded with chorionic villi and decidual cells.

ISH of *SHH*, *SOX9*, and *SOX2* revealed the interesting location of this OT and suggested that this tumor was an OT bud. The primitive glandular structures that expressed *SHH* resembled the endoderm of a 3-week embryo. These structures may differentiate into somatic tissues in association with many other genes as the tumor grows [8–11]. The region where *SHH* and *SOX2* were co-expressed may be where neural stem cells may develop, and the location where *SHH* and *SOX9* were co-expressed may be where cartilage formation would occur in future development [9, 11]. We speculated that the tumor could have eventually differentiated into a larger, mature teratoma with two or three germ layers; however, it is not certain exactly which components of the tumor would differentiate into which mature tissues. To determine such changes would require further analysis of other genes involved in differentiation and maturation.

From the formalin-fixed sections, we were able to extract the RNAs involved in embryonic morphogenesis and to obtain RNA signals involved in differentiation and maturation. Therefore, formalin-fixed sections are useful for gene analysis, and FFPE samples, including very small lesions, are extremely valuable and necessary for the study of tumorigenesis.

We believe that the 2 × 0.8 mm lesion is the smallest OT reported in the available literature in English. Its morphological characteristics and ISH identification of the three genes involved in maturation and differentiation suggest that the abnormal oocytes in some OTs (mature or immature) turn into tumor cells, which, when the tumor is small, may consist of immature cells that, while the tumor is growing, form a cascading network involving not only these three genes but also various other genes and epigenomes involved in embryonic morphogenesis. This development could cause these tumor cells to differentiate and mature into three germ layers, thereby becoming larger mature (rarely immature) teratomas. Although we observed the expression of the three genes in only one small OT, our findings are encouraging enough to promote further study of small teratomas, which may shed light on elucidating the pathogenesis of OTs through pathological study of gene expression involved in maturation and differentiation of these tumors.

Abbreviations

OT: ovarian teratoma

ISH: *in situ* hybridization

FFPE: formalin-fixed paraffin-embedded

SCTAT: sex cord tumor with annular tubules

Declarations

Ethics approval and consent to participate

The patients at admission to Musashino Red Cross Hospital, Shonan Kamakura General Hospital and Doai Memorial Hospital received the information that the patient's surplus biological material can be used for research, unless they don't consent (opt out). The patients examined in this study provided informed consent to publish this report, and this study was approved by the Institutional Review Board of Musashino Red Cross Hospital, Shonan Kamakura General Hospital and Doai Memorial Hospital.

Consent for publication

Informed consent to publish this report was obtained from the patients before writing this report.

Availability of data and materials

Not applicable. Several unstained slides (one of serial sections labeled slides 1–50) are preserved at 4°C and available (tissue sample collection 2481, Shonan Kamakura Hospital).

Competing interests

None declared.

Funding

None declared

Authors' contributions

ST conceived the idea and wrote the initial draft of the manuscript. US, HK, JI, HY, KO, and MN observed the slides and contributed to the interpretation of data. HK and MN performed RNA extraction and RNA ISH. RY was the attending physician for this patient. All authors discussed the results and approved the final manuscript.

Acknowledgments

We thank Professor Masafumi Muratani (Department of Genome Biology, Faculty of Medicine, University of Tsukuba, and Tsukuba Transborder Medical Center) for his kind advice and the support for RNA sequencing. The authors would like to thank Enago (www.enago.jp) for the English language review.

References

1. Prat J, Nogales FF, Cao D, Vang R, Carinelli SG, Zaloudek CJ. Germ cell tumours. In: Kurman RJ, Carcangiu ML, Herrington CS, Young RH, editors. WHO Classification of Tumours of Female Reproductive Organs. Lyon: IARC; 2014. p. 57-62.
2. Talerman A, Vang R. Teratoma. In: Kurman RJ, Ellenson LH, Ronnet BM, editors. Blaustein's Pathology of the Female Genital Tract. 6th edn. New York: Springer; 2011. p. 869-91.
3. Thomson JA, Itskovitz-Eldor J, Shapiro SS, Waknitz MA, Swiergiel JJ, Marshall VS, et al. Embryonic stem cell lines derived from human blastocysts. Science. 1998;282:1145-47.
4. Kudo M, Teshima S, Kishi H. A case report of small teratoma of the ovary. Jpn J Diagn Pathol. 2019;36:296-301 (Abstract in English).
5. Belder N, Coskun Ö, Erdogan BD, Ilk O, Savas B, Ensari A, et al. From RNA isolation to microarray analysis: comparison of methods in FFPE tissues. Pathol Res Pract. 2016;212:678-85.
6. Sha Y, Phan JH, Wang MD. Effect of low-expression gene filtering on detection of differentially expressed genes in RNA-seq data. In: 37th Annu Int Conf of the IEEE Eng Med Biol Soc (EMBC). 2015;2015:6461-64.
7. Zhou Y, Zhou B, Pache L, Chang M, Khodabakhshi AH, Tanaseichuk O, et al. Metascape provides a biologist-oriented resource for the analysis of systems-level datasets. Nat Commun. 2019;10:1523.
8. Carlson BM. Human Embryology and Developmental Biology. 6th edn. St. Louis: Elsevier; 2018.
9. Ferri A, Favaro R, Beccari L, Bertolini J, Mercurio S, Nieto-Lopez F, et al. Sox2 is required for embryonic development of the ventral telencephalon through the activation of the ventral determinants Nkx2.1 and Shh. Development. 2013;140:1250-61.
10. Yamamizu K, Schlessinger D, Ko MSH. Sox9 accelerates ESC differentiation to three germ layer lineages by repressing Sox2 expression through P21 (WAF1/CIP1). Development. 2014;141:4254-66.
11. Park J, Zhang JJ, Moro A, Kushida M, Wegner M, Kim PC. Regulation ofSox9 by Sonic Hedgehog (Shh) is essential for patterning and formation of tracheal cartilage. Dev Dyn. 2010;239:514-26.
12. Wang F, Flanagan J, Su N, Wang LC, Bui S, Nielson A, et al. RNAscope: a novel in situ RNA analysis platform for formalin-fixed, paraffin-embedded tissues. J Mol Diagn. 2012;14:22-9.
13. Yanai-Inbar I, Scully RE. Relation of ovarian dermoid cysts and immature teratomas: an analysis of 350 cases of immature teratoma and 10 cases of dermoid cyst with microscopic foci of immature tissue. Int J Gynecol Pathol. 1987;6:203-12.
14. Ayhan A, Bukulmez O, Genc C, Karamursel BS, Ayhan A. Mature cystic teratomas of the ovary: case series from one institution over 34 years. Eur J Obstet Gynecol Reprod Biol. 2000;88:153-7.

15. Dabner M, McCluggage WG, Bundell C, Carr A, Leung Y, Sharma R, et al. Ovarian teratoma associated with anti-N-methyl D-aspartate receptor encephalitis: a report of 5 cases documenting prominent intratumoral lymphoid infiltrates. Int J Gynecol Pathol. 2012;31:429-37.
16. Manivel JC, Dehner LP, Burke B. Ovarian tumorlike structures, biovular follicles, and binucleated oocytes in children: their frequency and possible pathologic significance. Pediatr Pathol. 1988;8:283-92

Figures

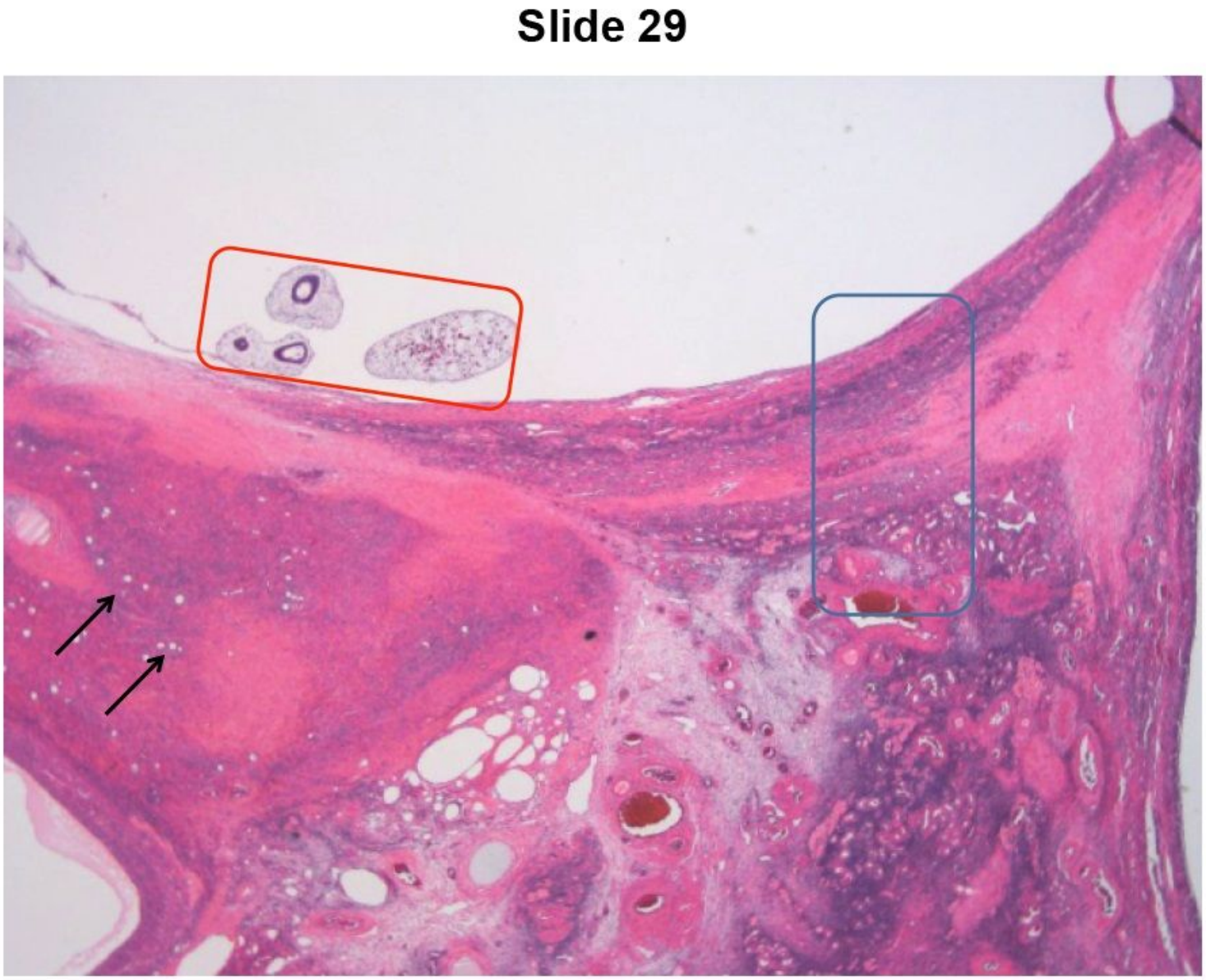

Figure 1

For RNA extraction, the sample (2 × 0.8 mm ovarian teratoma) was scraped with a needle tip from the unstained slides 26–28 (inside the red frame). The bulk tissue (control) was scraped from the oocyte-free

site of the ovary of the same unstained slides (inside the blue frame). The primary follicles are indicated by an arrow. The specimen pictured was slide 29 and stained with hematoxylin and eosin for reference

Figure 2

Hematoxylin and eosin-stained sections of the ovarian teratoma (OT). **a** An OT bud, 2 × 0.8 mm in size, was found protruding on the inner surface of the atretic follicle. The OT consisted of two nodules, 0.6 × 0.8 mm and 1.3 × 0.8 mm in size. Scale bar, 1 mm. **b** Components of the OT included a primitive glandular structure composed of dense overlapping high columnar cells and flat cells, another primitive glandular structure composed of dense columnar cells, small spindle-shaped to cuboidal cells in the area around these two structures, and one layer of flat cells covering the tumor surface. **c** The small spindle-shaped to cuboidal cells were densely or sparsely distributed, and the sinus-like structures contained red blood cells. **d** The glandular structure in the lower portion of the OT was long and tubular, and the center was narrowed and bent. **e** The lower glandular structure appeared to be two structures, but they were actually connected as one. Cord-like structures were mixed with coarsely distributed spindle-shaped to cuboidal cells (arrows)

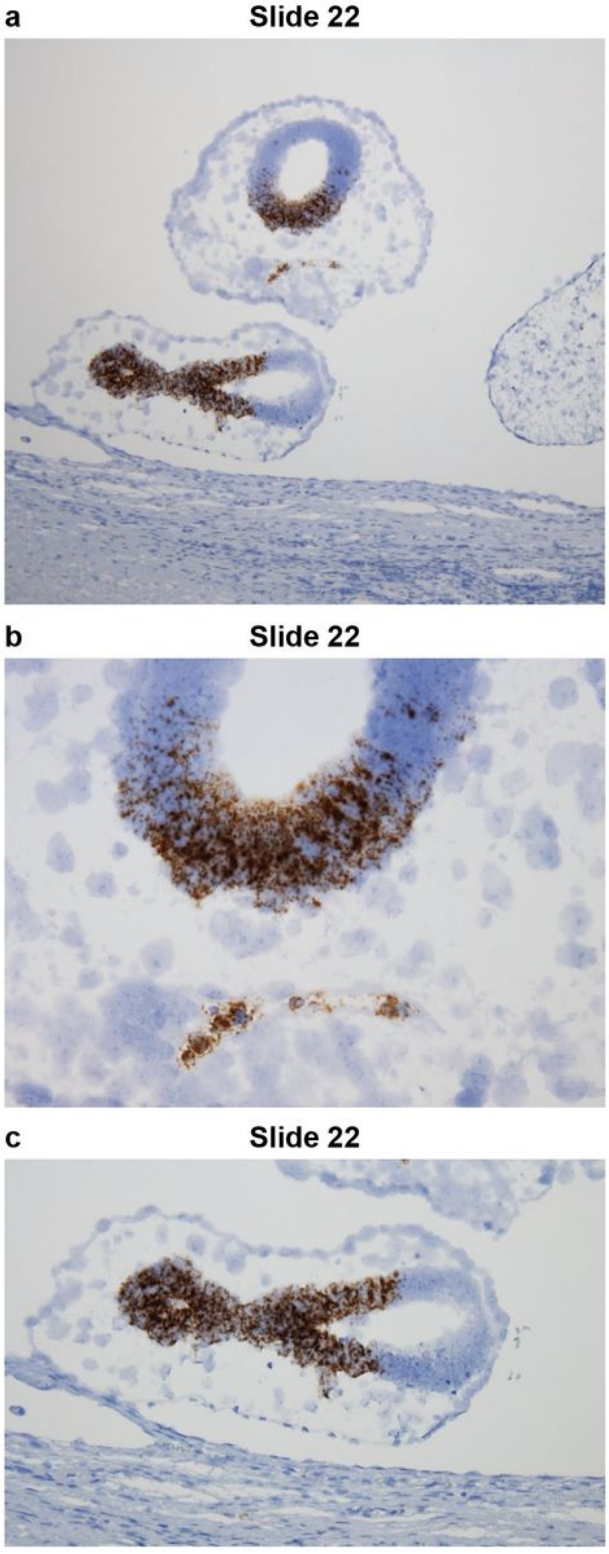

Figure 3

SHH RNA *in situ* hybridization (ISH). **a** *SHH* was highly expressed in the two primitive glandular structures and in the sinus-like structures formed by spindle cells. High signals were observed in 33% of the upper structure and in 75% of the lower structure. **b** The cord-like arrangement showed intense staining for the gene probe. *SHH* expression was not confirmed in mesoderm-like cells. **c** *SHH* signals were absent in the right side of the lower glandular structure

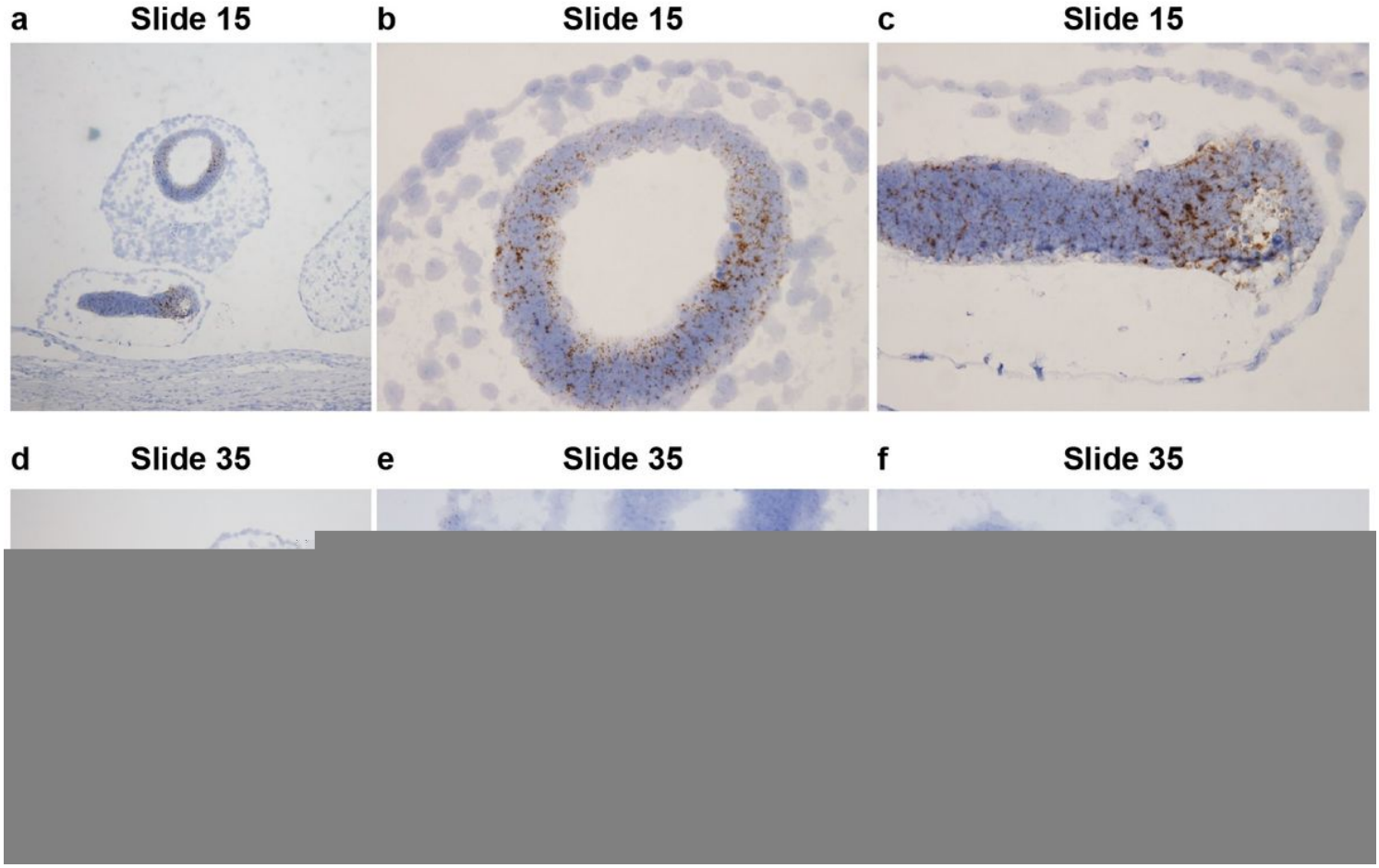

Figure 4

In situ hybridization (ISH) with *SOX2* RNA (**a–c**) and *SOX9* RNA ISH (**d–f**). **a** A low-power view shows the distribution of *SOX2* in the two primitive glandular structures. **b** In a high-power view, in the upper structure, *SOX2* was diffusely distributed, whereas flat-to-cuboidal cells on the tumor surface and the mesoderm-like cells did not react with the probe. **c** In a high-power view, in the lower structure, *SOX2* was diffusely distributed. **d** In a low-power view, *SOX9* was clearly detected with medium intensity in cord-like structures, where it also hybridized with the *SHH* probe (**Fig. 3b**). **e** In a high-power view, *SOX9* was not distributed in the upper structure, whereas the probe was detected in cord-like structures with medium intensity and in mesoderm-like cells and flat-to-cuboidal surface cells with low intensity (arrows). **f** In a high-power view, *SOX9* was distributed in the sinus-like structures and mesoderm-like cells (arrow) with low to medium intensity

Supplementary Files

This is a list of supplementary files associated with this preprint. Click to download.

- FCimage221.jpg